

## PRELIMINARY STUDIES ON HYDROXYAPATITE DOPED WITH EUROPIUM

Carmen Steluța CIOBANU<sup>1</sup>, Ecaterina ANDRONESCU<sup>2</sup>, Bogdan Ștefan VASILE<sup>3</sup>, Roxana TRUȘCĂ<sup>4</sup>, Daniela PREDOI<sup>5</sup>

*Scopul acestei lucrări constă în prepararea și caracterizarea hidroxiapatitei pure (HAp) și dopată cu europiu (Eu<sup>3+</sup>, Eu:HAp). Nanopulberile au fost obținute prin coprecipitare și caracterizate prin difracție de raze X (DRX), microscopie electronică de baleaj (MEB), spectroscopie în infraroșu cu transformata Fourier (FTIR) și microscopie electronică în transmisie (TEM). Rezultatele obținute pun în evidență faptul că Eu<sup>3+</sup> a fost înglobat cu succes în structura hidroxiapatitei. Rezultatele preliminare de DRX pun în evidență faptul că structura cristalină a nanopulberilor de Eu:HAp este asemănătoare cu structura hexagonală a hidroxiapatitei și că dimensiunea medie a particulelor variază între 10 și 20nm.*

*The aim of this paper is the preparation and characterization of pure hydroxyapatite (HAp) and HAp doped with europium (Eu<sup>3+</sup>, Eu:HAp). The nanopowders were obtained by co-precipitation method and analyzed through X-ray diffraction (XRD) scanning electron microscopy (SEM), infrared spectroscopy (FT-IR) and transmission electron microscopy (TEM). The results indicate that Eu<sup>3+</sup> has been successfully doped into the framework of HAp. The preliminary XRD results reveal that the obtained Eu:HAp particles are well assigned to the hexagonal lattice structure of the hydroxyapatite phase and the mean crystallite size varies between 10 and 20 nm.*

**Keywords:** hydroxyapatite, nano-particles, europium, co-precipitation

### 1. Introduction

The first structural identifications of biominerals using X-ray diffraction were obtained by De Jong in 1926 [1]. He established that calcium phosphate biominerals of vertebrates corresponded to an apatite structure and since that time bone mineral has been frequently identified as hydroxyapatite (HAp): Ca<sub>10</sub>(PO<sub>4</sub>)<sub>6</sub>

<sup>1</sup> Eng., Faculty of Applied Chemistry and Material Science, University POLITEHNICA of Bucharest; Scientific research assistant, National Institute for Physics of Materials, Romania

<sup>2</sup> Prof., Faculty of Applied Chemistry and Material Science, University POLITEHNICA of Bucharest, Romania

<sup>3</sup> Eng., Faculty of Applied Chemistry and Material Science, University POLITEHNICA of Bucharest, Romania

<sup>4</sup> Eng., METAV Research & Development, Bucharest, Romania

<sup>5</sup> Senior Researcher, National Institute for Physics of Materials, Bucharest, Romania, e-mail:dpredoi68@gmail.com

(OH)<sub>2</sub> which was later considered to crystallize in the hexagonal system (space group *P*6<sub>3</sub>/*m*).

HAp in the form of a non-stoichiometric, ion-substituted and calcium-deficient hydroxyapatite (commonly referred to as “biological apatite”), are present in bones, teeth, tendons of mammals, giving these organs stability, hardness and function [5-7]. Synthetic apatites can be prepared by several methods (precipitation under conditions of constant or changing composition, hydrolysis, solid/solid reaction at high temperature, hydrothermal methods) the type of which determines the amount and kind of substitution in the apatite. Numerous apatite-type compounds are known to exhibit good luminescence characteristics [9-11]. Europium is a well-known and thoroughly investigated active element in the field of lighting and display [12]. Luminescent properties depend strongly on the crystal structure of the host materials. HAp crystals have been widely used in delivery systems for genes [13], proteins [14] and various drugs [15-16] due to their non-toxicity and excellent biocompatibility, as have been experimentally proven by recent reports [17-20]. Europium is a luminescent agent with great bio-compatibility and is ideal for implantation and clinical application [23].

In this study, europium doped hydroxyapatite with an atomic ratio Eu/(Eu +Ca) equal with 0% and 20% were synthesized by co-precipitation. The structure, morphology, and optical properties were characterized by X-ray diffraction (XRD), scanning electron microscopy (SEM), transmission electron microscopy (TEM) and Fourier transform infrared (FT-IR) spectroscopy.

## 2. Experimental procedure

### 2.1. Sample preparation

All the reagents for synthesis including ammonium dihydrogen phosphate [(NH<sub>4</sub>)<sub>2</sub>HPO<sub>4</sub>], calcium nitrate [Ca(NO<sub>3</sub>)<sub>2</sub>×4H<sub>2</sub>O], and europium nitrate [Eu(NO<sub>3</sub>)<sub>3</sub>×6H<sub>2</sub>O] (Alpha Aesar) were purchased without further purification. Europium-doped hydroxyapatite (Eu:HAp) was obtained at 80°C. The Eu:HAp was obtained by mixing Eu(NO<sub>3</sub>)<sub>3</sub>×6H<sub>2</sub>O, Ca(NO<sub>3</sub>)<sub>2</sub>×4H<sub>2</sub>O and (NH<sub>4</sub>)<sub>2</sub>HPO<sub>4</sub> in deionized water together (Ca/P molar ratio: 1.67 and an atomic ratio Eu/(Eu +Ca) equal with 0% and 20%) and stirred until a homogeneous solution was formed. The pH was adjusted to 9 using 2M NH<sub>3</sub>. The obtained precipitate was filtered and washed for several times with deionized water. The resulting material was dried at 80°C for 72h.

## 2.2. Sample characterization

The samples were characterized for phase content by X-ray diffraction (XRD) with a Bruker D8-Advance X-ray diffractometer in the scanning range  $2\theta (^{\circ}) = 15 - 90$  using  $\text{CuK}_{\alpha 1}$  incident radiation.

Particle morphologies were observed with a scanning electron microscope QUANTA INSPECT F at 30 kV accelerating voltage. The SEM studies were performed on powder samples. For the elemental analysis the electron microscope was equipped with an energy dispersive X-ray attachment (EDAX/2001 device).

The functional groups present in the prepared powder were identified by FTIR (Spectrum BX Spectrometer). For this 1% of the powder was mixed and ground with 99% KBr. Tablets of 10 mm diameter for FTIR measurements were prepared by pressing the powder mixture at a load of 5 tons for 2 min and the spectrum was taken in the range of 400 to 2000  $\text{cm}^{-1}$  with resolution 4 and 128 times scanning.

The structure and morphology of the samples were studied using transmission electron microscopy. The micrographs were obtained using a Tecnai<sup>TM</sup> G<sup>2</sup> F30 S-TWIN transmission electron microscope (from FEI - The Netherlands), equipped with STEM/HAADF detector, EDS (Energy dispersive X-ray Analysis and EFTEM - EELS (Electron energy loss spectroscopy), with the following characteristics: acceleration voltage of 300 KV obtained from a Shottky Field emitter; TEM point resolution of 2 Å; TEM line resolution of 1.02 Å; The specimen for TEM imaging was prepared from the particles suspension in ethanol. A drop of well-dispersed supernatant was placed on a carbon – coated 200 mesh copper grid, followed by drying the sample at ambient conditions before it is attached to the sample holder on the microscope.

## 3. Results and discussions

### 3.1. Phase composition

Fig. 1 shows the XRD patterns of pure HAp and Eu:HAp with  $\text{Eu}/(\text{Eu} + \text{Ca}) = 20\%$ . Fig. 1A shows the typical diffraction peaks of hexagonal  $\text{Ca}_{10}(\text{PO}_4)_6(\text{OH})_2$ , which can be indexed as the standard data (JCPDS No. 09-0432). For the Eu:HAp sample in Fig. 1B, the characteristic diffractions of HAp is still obvious, and no other phase related with the doped  $\text{Eu}^{3+}$  can be detected. This results indicate that  $\text{Eu}^{3+}$  has been successfully doped into the framework of HAp. The XRD patterns reveal that the structure of pure HAp and Eu:HAp belongs to the hexagonal  $P6_3/m$  space group (JCPDS No. 09-0432). As the  $\text{Eu}/(\text{Eu} + \text{Ca})$  concentration increases to 20% the peaks broaden, suggest that the doping inhibits the HAp crystal growth and/or causes lattice perturbations (microstrain). One can observe also an increased background intensity in this pattern, which is

presumably due to an amorphous component. The determination of the average crystallite size by XRD method is based on the Scherrer equation [24]:

$$D_{\text{crystallite}} = K\lambda/B \cos\theta \quad (1)$$

where  $D_{\text{crystallite}}$  is the averaged length of coherence domains (that is of perfectly ordered crystalline domains) taken in the direction normal to the lattice plane that corresponds to the diffraction line taken into account,  $B$  is the line broadening due to the small crystallite size,  $\lambda$  is the wavelength of X-rays,  $\theta$  is the Bragg angle, and  $K$  a constant related to crystallite shape and to the definition of  $B$  (integral breadth or full width at half maximum). The following results were obtained for the mean crystallite size:  $D=18 \text{ nm } (\pm 0.1)$  for pure HAp and  $D=12 \text{ nm } (\pm 0.5)$  for Eu:HAp with  $\text{Eu}/(\text{Eu} + \text{Ca})=20\%$ .

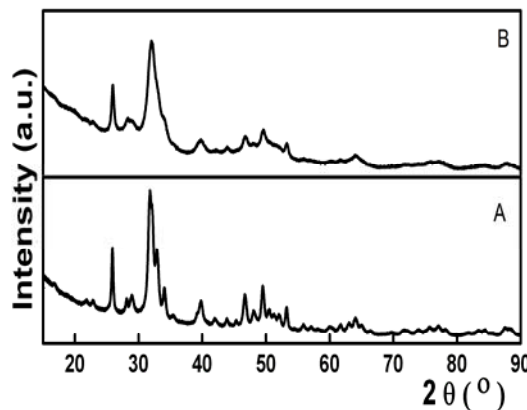


Fig. 1. XRD patterns of pure HAp (A); Eu:HAp with  $\text{Eu}/(\text{Eu} + \text{Ca})=20\%$  (B)

Table 1

Cell parameter of pure HAp, Eu:HAp with  $\text{Eu}/(\text{Eu} + \text{Ca})=20\%$

| Cell parameters (Å) | Pure HAp | Eu:HAp with $\text{Eu}/(\text{Eu} + \text{Ca})=20\%$ |
|---------------------|----------|--|
| a                   | 9.4431   | 9.4185   |
| c                   | 6.8754   | 6.8692   |

### 3.2. Samples morphology

SEM images of pure HAp are presented in Fig. 2 (Fig. 2A), and Eu:HAp (Fig. 2B). SEM images provide the direct information about the morphology of the as-prepared samples. The micrographs reveal that the powders have the

tendency to form agglomerates, most probably, due to the low particle size. The results suggest that the doping of  $\text{Eu}^{3+}$  has little influence on the morphology of pure HAp. The EDAX spectrum of Eu:HAp (Fig. 2D) confirms the presence of calcium (Ca), phosphor (P), oxygen (O) and europium (Eu) in the Eu:HAp sample.

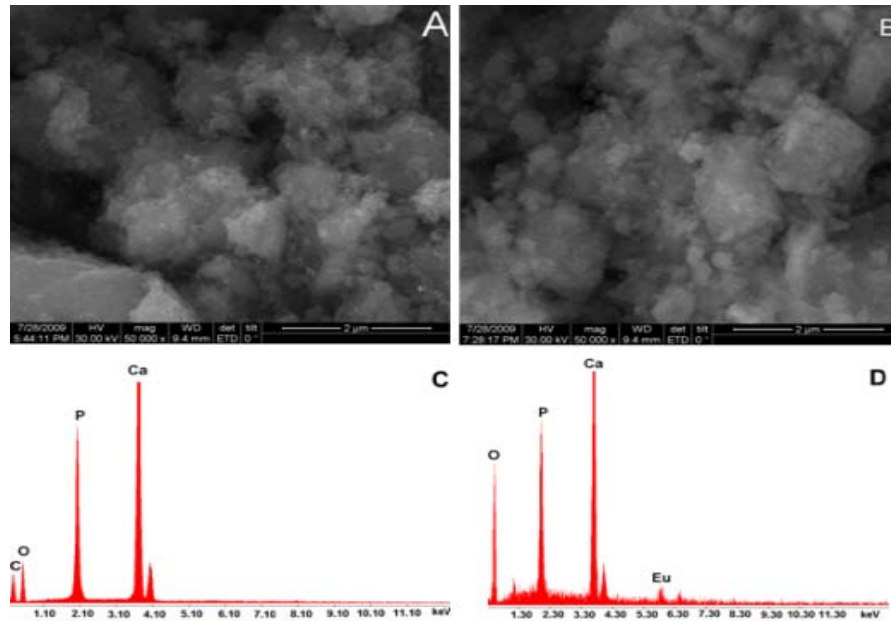


Fig. 2. SEM images of pure HAp (A), Eu:HAp with  $\text{Eu}/(\text{Eu} + \text{Ca}) = 20\%$  (B); EDAX spectrum of pure HAp (C), Eu:HAp with  $\text{Eu}/(\text{Eu} + \text{Ca}) = 20\%$  (D)

### 3.3. Fourier Transform Infrared Spectroscopy

The FT-IR spectra of pure HAp (A), Eu:HAp with  $\text{Eu}/(\text{Eu} + \text{Ca}) = 20\%$  (B) are presented in Fig. 3. The peaks of  $1032 \text{ cm}^{-1}$  correspond to the asymmetric stretching vibration of  $\text{PO}_3^{4-}$ , and the peaks of  $600, 560 \text{ cm}^{-1}$  in pure HAp (Fig. 3A) and the peaks of  $604, 563 \text{ cm}^{-1}$  (Fig. 3B) correspond to the bending vibration. The peak at  $1419 \text{ cm}^{-1}$  in Fig. 3B indicates that the samples contained a small amount of  $\text{CO}_3^{2-}$ . The vibrational spectrum position of the anion group was influenced. In Eu-HA, the calcium ions were replaced by europium ions. In Fig. 3A, the wave number of OH in pure HAp are  $1565 \text{ cm}^{-1}$ , and the wave number of OH in Eu:HAp are  $1570 \text{ cm}^{-1}$  in Fig. 3B. We can see that the wave number of the OH<sup>-</sup> band increases with the radii of cations of hydroxyapatite owing to the increase in the hydrogen bond distance OH<sup>-</sup>.

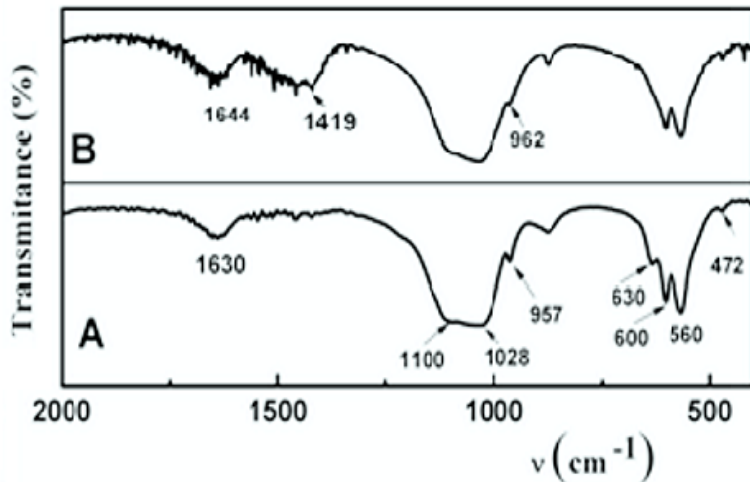


Fig. 3. FT-IR spectra of pure HAp (A), Eu:HAp with  $\text{Eu}/(\text{Eu} + \text{Ca}) = 20\%$  (B)

### 3.4. Transmission electron microscopy (TEM)

The TEM micrographs of Eu:HAp is presented in Fig. 4. TEM images provide the direct information about the morphology of the as-prepared samples. The micrographs reveal that the powders have the tendency to form soft agglomerates, most probably, due to the low particle size. Fig. 4 reveals the formation of nanocrystalline HAp wires with a diameter in length varying from 20 to 30 nm and a width varying from 5 to 12 nm. The morphology is also different as we can observe in the Fig. 4(A), the nanowires are smooth, with the same diameter from one end to another. In the other sample, Fig. 4(B) probably due to the addition of Eu, the morphology changes, thus, the diameter varying along the length of nanowires. The results suggest that the doping of  $\text{Eu}^{3+}$  has a little influence on the morphology of the samples.

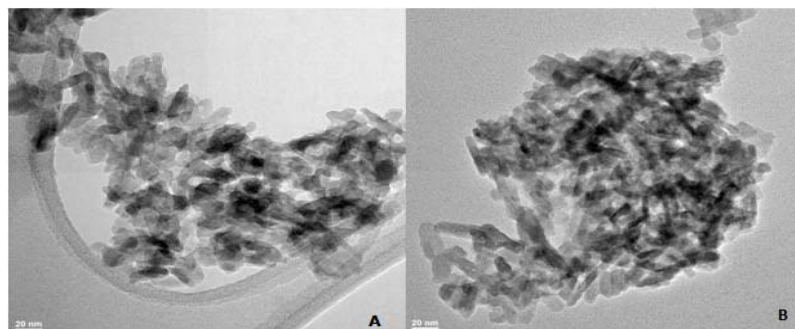


Fig. 4. TEM micrographs of of pure HAp (A), Eu:HAp with  $\text{Eu}/(\text{Eu} + \text{Ca}) = 20\%$  (B)

#### 4. Conclusions

The europium-doped HAp were synthesized at 80°C by co-precipitating a mixture of  $\text{Ca}^{2+}$  and  $\text{Eu}^{3+}$  ions by phosphate ions in water medium. The preliminary DRX studies have shown that  $\text{Eu}^{3+}$  has been successfully doped into HAp. The results reveal that the obtained Eu:HAp particles are well assigned to the hexagonal lattice structure of the hydroxyapatite phase. The europium-doped HAp show a potential application in various fields based on their nano-sized and luminescent properties.

#### Acknowledgments

The work has been funded by the Sectoral Operational Programme Human Resources Development 2007-2013 of the Romanian Ministry of Labour, Family and Social Protection through the Financial Agreement POSDRU/6/1.5/S/19 and PNCDI II 71-097/2007, Core Program contract PN09-45.

#### R E F E R E N C E S

- [1] *W.F. De Jong, J. Bouman, J.J. De Lange*, “X-ray photography of zero-order reciprocal net planes of a crystal”, *Physica*, **Vol. 5**, Iss. 3, 1938, pp. 188-192
- [2] *P. Christel, A.T. Klein, Y. Abe, H. Hosono, K. de Groot*, “Comparison of calcium phosphate glass ceramics with apatite ceramics implanted in bone. An interface study—II”, *Biomaterials*, **Vol. 8**, Iss. 3, 1987, pp. 234-236
- [3] *W. Bonfield*, “Composites for bone replacement”, *Jornal of Biomedical Engineering*, **Vol. 10**, Iss. 6, 1988, pp. 522-526
- [4] *M. Prodana, D. Bojin, D. Ioniță*, “Effect of hydroxyapatite on interface properties for alloy/biofluid”, *U.P.B. Sci. Bull., Series B*, **Vol. 71**, Iss. 4, 2009, pp. 89
- [5] *H.A. Lowenstam, S. Wein*, “On biomineralization”, Oxford University Press, 1989
- [6] *M. Vallet-Regi, J. M. González-Calbet*, “Calcium phosphates as substitution of bone tissues”, *Prog Solid State Sci.*, **Vol. 32**, 2004, pp. 1-31

- [7] *S. Weiner, L. Addadi*, “Design strategies in mineralized biological materials”, *J. Mater. Chem.* **Vol. 7**, 1997, pp. 689–702
- [8] *D. M. Liu, T. Troczynski, W. J. Tseng*, “Aging effect on the phase evolution of water-based sol-gel hydroxyapatite”, *Biomaterials*, **Vol. 23**, Iss. 4, 2002, pp. 1227-1236
- [9] *S. Weiner, H.D. Wagner*, “The material bone: structure-mechanical function relations”, *Annual Rev. of Mat. Sci.*, **Vol. 28**, 1998, pp. 271-298
- [10] *T. J. Issacs*, “A Study of Eu<sup>3+</sup> Fluorescence in Some Silicate Oxyapatites”, *J. Electrochem. Soc.*, **Vol. 120**, 1973, pp. 654
- [11] *C. Feldmann, T. Justel, C.R. Ronda, P.J. Schmidt*, “Inorganic Luminescent Materials - 100 Years of Research and Application”, *Adv. Funct. Mater.*, **Vol. 13**, Iss. 7, 2003, pp. 511
- [12] *L. Boyer, B. Piriou, J. Carpena, J.L. Lacout*, “Study of sites occupation and chemical environment of Eu in phosphate-silicates oxyapatites by luminescence”, *J. Alloys Compd.*, **Vol 311**, 2000, pp. 143–152
- [13] *S. Ekambaram, K.C. Patil, M. Maaza*, “Synthesis of lamp phosphors: facile combustion approach”, *J. Alloys Compd.*, **Vol. 393**, 2005, pp. 81-92
- [14] *P. Sibilla, A. Sereni, G. Aguiari, M. Banzì, E. Manzati, C. Mischiati*, “Effects of a Hydroxyapatite-based Biomaterial on Gene Expression in Osteoblast-like Cells”, *J. Dent. Res.*, **Vol. 85**, 2006, pp. 354-358
- [15] *S. Dasgupta, A. Bandyopadhyay, S. Bose*, “Reverse micelle-mediated synthesis of calcium phosphate nanocarriers for controlled release of bovine serum albumin”, *Acta Biomater.*, **Vol. 5**, Iss. 8, 2009, pp. 3112-3121
- [16] *T.Y. Liu, S.Y. Chen, D.M. Liu, S.C. Liou*, “On the study of BSA-loaded calcium-deficient hydroxyapatite nano-carriers for controlled drug delivery”, *J. Control Release*, **Vol. 107**, 2005, pp. 112-121
- [17] *B. Palazzo, M. Iafisco, M. Laforgia, N. Margiotta, G. Natile, C.L. Bianchi*, “Biomimetic Hydroxyapatite/drug Nanocrystals as Potential Bone Substitutes with Anti-tumour Drug Delivery and Release Properties”, *Adv. Funct. Mater.*, **Vol. 17**, 2007, pp. 2180-2188
- [18] *X. Zhu, O. Eibl, L. Scheideler, J. Geis-Gerstorfer*, “Characterization of nano hydroxyapatite/collagen surfaces and cellular behaviors”, *J. Biomed. Mater. Res. A*, **Vol. 79A**, 2006, pp. 114-127
- [19] *X. Zhu, O. Eibl, C. Berthold, L. Scheideler, J. Geis-Gerstorfer*, “Structural characterization of nanocrystalline hydroxyapatite and adhesion of pre-osteoblast cells”, *Nanotechnology*, **Vol. 17**, 2006, pp. 2711
- [20] *Y. R. Cai, Y. K. Liu, W. Q. Yan, Q. H. Hu, J. H. Tao, M. Zhang, Z. L. Shi, R. K. Tang*, “Role of hydroxyapatite nanoparticle size in bone cell proliferation”, *J. Mater. Chem.*, **Vol. 17**, 2007, pp. 3780-3787
- [21] *W. Andreoni, D. Scharf, P. Giannozzi*, “Low-temperature structures of C<sub>4</sub> and C<sub>10</sub> from the Car–Parrinello method: singlet states”, *Chemical Physics Letters*, **Vol. 173**, Iss. 5-6, 1990, pp. 449-455
- [22] *A. Doat, F. Pellé, A. Lebugle*, “Europium-doped calcium pyrophosphates: allotropic forms and photoluminescent properties”, *J. Solid State Chem.*, **Vol. 178**, Iss. 7, 2005, pp. 2354-2362
- [23] *A. Doat, M. Fanjul, F. Pellé, E. Hollande, A. Lebugle*, “Europium-doped bioapatite: a new photostable biological probe internalizable by human cells”, *Biomaterials*, **Vol. 24**, Iss. 19, 2003, pp. 3365-3371
- [24] *P. Scherrer*, “Bestimmung der Größe und der inneren Struktur von Kolloidteilchen mittels Röntgenstrahlen. Nachrichten von der Gesellschaft der Wissenschaften zu Göttingen”, *Mathematisch-Physikalische Klasse*, **Vol. 2**, 1918, pp. 98.